Journal of
Mechanical
Science and
Technology

Journal of Mechanical Science and Technology 21 (2007) 1512~1517

Prediction of failure in tube hydroforming process using a damage model

G. H. Majzoobi[1,*], F. Freshteh Saniee[2], A. Shirazi[2]

[1]*Mechanical Engineering Department, Bu-Ali Sina University, Hamadan, Iran*
[2]*Mechanical Engineering Department, Bu-Ali Sina University, Hamadan, Iran*

(Manuscript Received May 31, 2007; Revised August 30, 2007; Accepted September 30, 2007)

Abstract

In tube hydroforming process (THP), two types of loading, internal pressure and axial feeding and in particular the combination of them, are needed to feed the material into the cavities of the die to form the workpiece into the desired shape. If the variation of pressure versus axial feeding is not determined properly, the workpiece may be buckled, wrinkled or burst during THP. The appropriate variation is normally determined by experiment which is expensive and time-consuming. In this work, numerical simulation using Johnson-Cook models for predicting the elasto-plastic response and the failure of the material are employed to obtain the best combination of internal pressure and axial feeding. The numerical simulations are examined by a number of experiments conducted in the present investigation. The results show very close agreement between the numerical simulations and the experiments, suggesting that the numerical simulations using Johnson-Cook material and failure models provide a valuable tool to examine the different parameters involved in THP.

Keywords: Tube hydroforming process (THP); Failure model; Internal pressure; Axial feeding

1. Introduction

Hydroforming is simply a metal process that relies on fluid pressure, usually oil or water, to shape the metal piece. First, the metal piece to be formed is placed in a blank holder between two punches. The blank holder and the punches are then moved next to the fluid filled specimen and pressure inside the specimen is increased to form the workpiece. The THP is schematically shown in Fig. 1. Typical components made by THP are illustrated in Fig. 2. As stated above, any improper selection of the combination of axial feeding and pressurizing the blank from inside may result in either buckling, due to excessive axial feeding, or bursting of the blank, due to the excessive pressure. Song *et al.* [1] have investigated the bursting failure in THP under combined internal pressure and independent axial feeding. They also introduced the Cockcroft and Latham's ductile failure criterion into a finite element analysis to predict the bursting failure of the workpiece. Yuan *et al.* [2, 3] studied the effects of loading path and length to diameter ratio on the number of wrinkles and part shape. They concluded that not all wrinkles were defects and that the key point in THP is to obtain useful wrinkles instead of dead wrinkles. In other words, if the loading path is selected properly, the wrinkles are useful and the part can be formed successfully with these wrinkles. Arbantes *et al.* [4] established a basic understanding of the THP of aluminum using LSDYNA hydro code. Li *et al.* [5] presented the characteristics of THP by determining how the stress state moves on the yield ellipse during

*Corresponding author. Tel.: +98 811 8257409, Fax.: +98 811 8257400
E-mail address: gh_majzoobi@yahoo.co.uk

the process. They showed that the stress state plays an important role during THP, determining the final shape of the components. Lianfa and Cheng [6] introduced a simple experimental tooling with internal pressure source used for evaluation of material formability in tube THP. Their tooling was able to establish required internal pressure in synchronization with axial load, through the little movement of the punch. Further works can be found in references [7] and [8]. In this work, numerical simulations are employed to determine the proper loading path for a successful calibration. It is tried to select proper material and failure models to predict the buckling, wrinkling and bursting phenomena which are usually occur in THP. The numerical simulations are carried out using LSDYNA hydro code. The validity of the simulations is then verified by conducting a number of tests with cylindrical specimens.

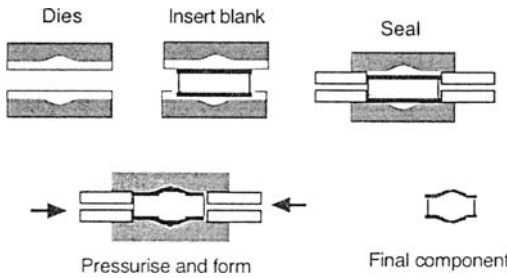

Fig. 1. A schematic view of hydroforming process sequence.

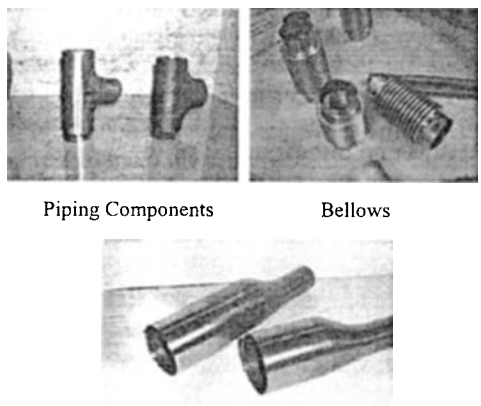

Fig. 2. Typical components made by hydroforming process.

1.2 Material and Failure models

The material model which is usually obtained from standard tensile tests can significantly affect the numerical simulations. One of the models which has gained more popularity over the past 20 years is the elasto-plastic model known as Johnson-Cook constitutive equation. The model in this work is expressed as follows:

$$\sigma = \left(A + B\varepsilon^{n}\right)\left(1 + CLn\dot{\varepsilon}^{*}\right)\left(1 - T^{*m}\right) \tag{1}$$

where A, B, C, n and m are constants and are determined by experiments carried out in this investigation. T^{*} is the homologous temperature defined as $T^{*} = (T - T_{room})/(T_{melt} - T_{room})$ in which T_{melt} and T_{room} are the melt and room temperature, respectively. The strain rate parameter $\dot{\varepsilon}^{*} = \dot{\varepsilon}/\dot{\varepsilon}^{0}$ is the non-dimensional strain rate for $\dot{\varepsilon}^{0} = 1.0s^{-1}$. One of the main problems in THP is prediction of failure of the blank piece which may occur before it is formed. In fact, the combination of pressure and the axial material feed which can be applied to the blank piece before it fails is of a great concern. This can be accomplished using finite element analysis along with a damage criterion known as Johnson-Cook failure model which is given as:

$$\varepsilon_{f} = \left(D_{1} + D_{2}\exp\left(D_{3}P/\bar{\sigma}\right)\right)\left(1 + D_{4}Ln(\dot{\varepsilon}^{*})\right)\left(1 + D_{5}T^{*m}\right) \tag{2}$$

where $D_{1} - D_{5}$ are the material constants and are determined by experiment. P is the hysdrostatic pressure and $\bar{\sigma}$ is the equivalent stress. According to Johnson-Cook model, failure occurs when the damage parameter, $D = \sum \Delta\varepsilon_{f}/\varepsilon_{f}$, reaches unity. $\Delta\varepsilon_{f}$ is the strain increment at each load increment and ε_{f} is the failure strain calculated from Eq. (2).

2. Material and specimens

The specimens are made of AISI 1010 steel which is widely used in industry and has a good formability subject to a proper heat treatment. Two types of materials, (i) as received and (ii) heat treated were used in the experiments. Both materials have the following properties:

$$\rho = 7830\ Kg/m^{3}, \quad E = 207\ GPa, \qquad \nu = 0.28$$

The stress-strain curves for the two materials were obtained by conducting a number of standard tensile tests using the universal servo-hydraulic testing device Instron. The curves are illustrated in Fig. 3. Using the curve fitting techniques, the constants of

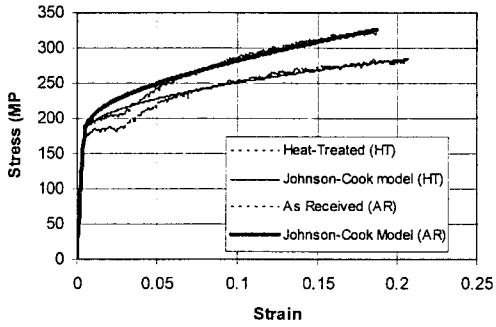

Fig. 3. True stress-strain curves for as received and heat treated materials.

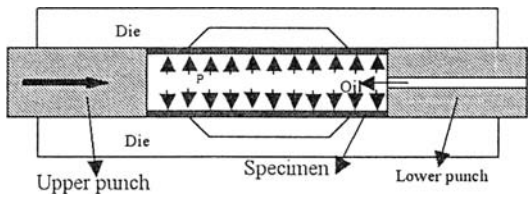

Fig. 4. The specimen, die and the punch assembly used in the experiments (not scaled).

the Johnson-Cook model were obtained as given below:

$A = 197.2\ MPa,\quad B = 375.6\ MPa,\quad n = 0.621$

For as received material

$A = 179.2\ MPa,\quad B = 242.2\ MPa,\quad n = 0.520$

For heat treated material

For the heat treatment, the specimens were heated at a temperature of $830\ ^0C$ and then were cooled in the furnace. As can be seen in the figure, the heat treatment has considerably softened the material and has slightly increased the elongation. In a separate work, the material constants for Johnson-Cook failure model (Eq. 2) were obtained for as received and heat treated materials and are given below:

$D_1 = -1.1,\ D_2 = 2.441,\ D_3 = -1.032,\ D_4 = 0,\ D_5 = 0$

For as received material

$D_1 = -0.988,\ D_2 = 2.441,\ D_3 = -1.032,\ D_4 = 0,\ D_5 = 0$

For heat treated material

Specimens are cylindrical with the inner and outer radii of 6 mm and 40 mm, respectively. The length of the specimens is 150 mm. The ends of the cylinders are made conical for sealing purposes. The specimen, die and the punch assembly are schematically illustrated in Fig. 4.

3. Numerical simulations and experiments

The numerical simulations are carried out using the LSDYNA hydro-code. The finite element model comprises the die, the punches and the specimen as shown in Fig. 4. Because of symmetry, only 1/4 of the cylindrical specimens is modeled for the simulations. The model consists of 1125 thin shell elements with 1216 nodes. The punches and dies are assumed to be rigid. The contact surfaces between the die and the specimen are defined by contact-automatic surface to surface elements. The coefficient of friction between the die and the specimens is taken as 0.18. The lower punch is kept fixed during THP and only the upper punch is allowed to move downward in direc-tion of the axis of symmetry. The variation of axial loading versus pressure called the loading path is typically shown in Figs. 5 to 8. The experiments are conducted using a THP assembly shown in Fig. 4. The axial feeding is supplied by a 60 tons servo-hydraulic testing machine, Instron and the internal pressure is supplied by an Enerpac type pump with a capacity of 40,000 psi (2000 bars). The experiments are carried out for both as received and heat treated specimens. The experiments comprise of the tests with only axial feeding to study the evolution of the wrinkles, the tests with only internal pressure to study the burst phenomenon in the specimens and the tests at different combinations of axial feeding plus in-ternal pressure.

4. Results and discussion

The as received and the heat treated specimens exhibited quite different behaviors during THP. A typical result is depicted in Fig. 5. In this figure, an as received and a heat treated specimen tested under the same loading path are compared. From the profiles shown in Fig. 5, it can be clearly observed that both specimens have undergone the same amount of deformation. However, while the as received speci-men was burst, the heat treated speci-men was remained perfect. As a matter of fact, heat treatment has increased the specimen's formability which is a vital requirement in metal forming pro-cesses. In most of the as received specimens, failure occurred before the material could take the form of the die cavity and the THP was completed. However, the

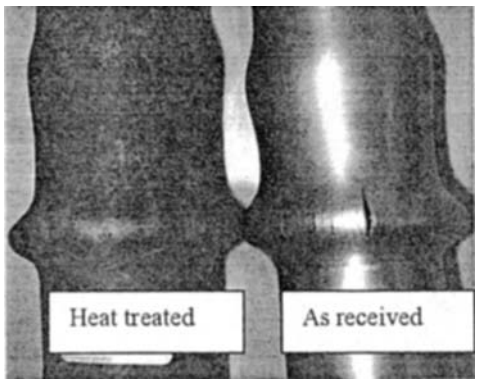

Fig. 5. The deformation in an as received and a heat treated specimen.

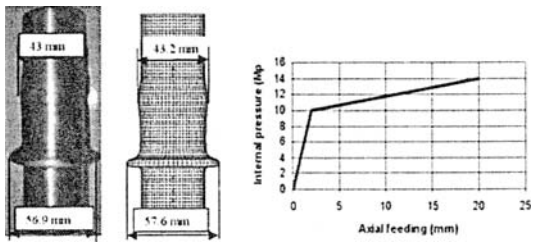

Fig. 6. The wrinkle produced by excessive axial feeding.

results for both types of specimens are given in the paper.

Two important issues are investigated in this work; (i) the validity of the material model and (ii) the validity of the failure model. The models were briefly discussed in section 2. The validity of the material model is examined by making comparisons between the profiles of the deformed specimens obtained from experiments and those predicted by numerical simulations under different loading paths. The results shown in Figs. 6 to 9 exhibit a remarkable agreement not only between the numerical and the experimental profiles of the deformed specimens but also between the dimensions of the profiles either. The loading path is also shown in each figure. These encouraging results are a good indication that the material model has been selected properly and its material constants have been determined accurately.

The validity of the failure model is investigated by making comparison between the failure of the specimens similar to the experiments with those predicted by numerical simulations. As discussed in section 2, in numerical simulations failure is assumed to occur when the damage parameter, $D = \sum \Delta\varepsilon_f / \varepsilon_f$,

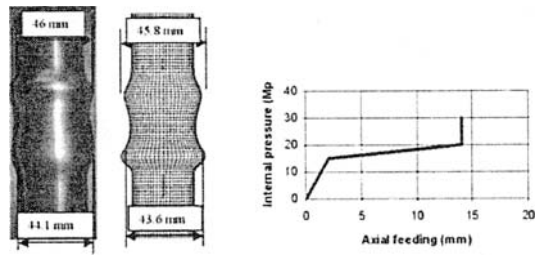

Fig. 7. A comparison between the numerical and experimental profiles evolution in an interrupted hydroforming test.

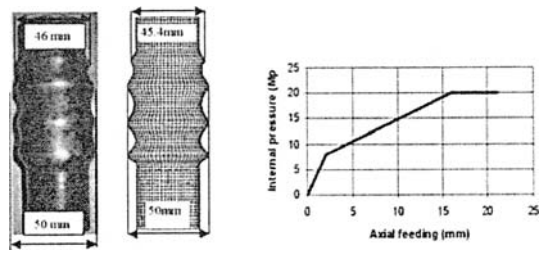

Fig. 8. The multy-wrinkles produced by an improper choice of a loading path.

exceeds 1 in an element. As soon as this happens, the deviatoric stresses are set to zero in the failed element and that element can no longer carry any tensile load. At this point, the calculations are terminated. The contours of the first principal deviatoric stress are used to locate the point of the onset of the failure in the specimen.

The results of failure simulations are compared with those obtained from the experiments in Figs. 10 to 13. Only half of the specimens in numerical simulations are shown in these figures. The burst element number is given in the figures. The simulations comprise of three distinct loading paths. Fig. 10 illustrates a hydroformed specimen under only axial feeding. The figure shows reasonable agreement between the experiment and the simulation. The interesting point is that the failure initiates from the same region which is located on the tip of the wrinkle produced by the axial feeding for both numerical simulation and the experiment. Fig. 11 shows the results for a specimen with only internal pressure. Again, a good agreement between the numerical and the experimental results is observed for the hydroformed specimen. Fig. 12 corresponds to the case where THP has been conducted under a combination of axial feeding and the internal pressure. Fig. 13 shows a successful calibration in which no failure has occurred and the material has completely filled the

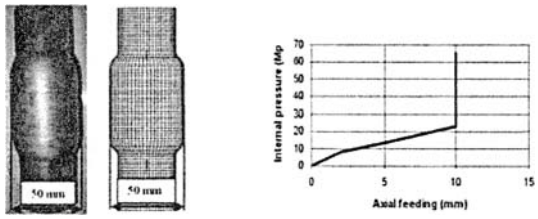

Fig. 9. A proper loading path in a successful calibration.

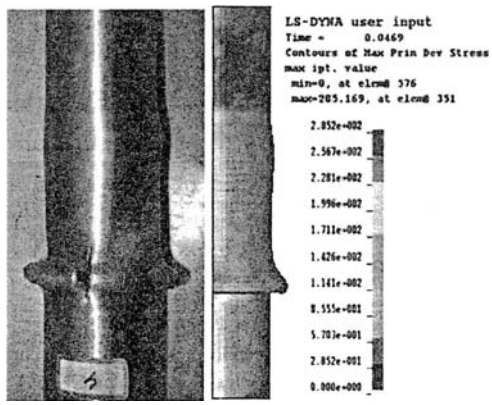

Fig. 10. Experimental and numerical predictions of bursting in a specimen with only axial feeding.

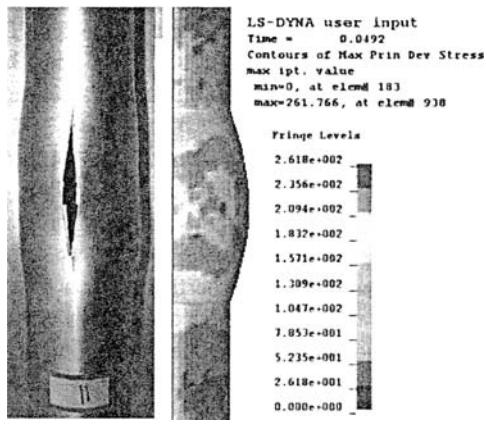

Fig. 11. Experimental and numerical predictions of bursting in a specimen with only internal pressure.

cavity of the die. The reasonable agreement between the numerical and the experimental results reveals that the Johnson Cook failure model can confidently be used for predicting the proper axial feeding and the pressurizing rates for a successful calibration. This saves the costs and reduces the time for the tests required in a THP process.

The experimental measurements and the numerical predictions for the axial movement of the punch and

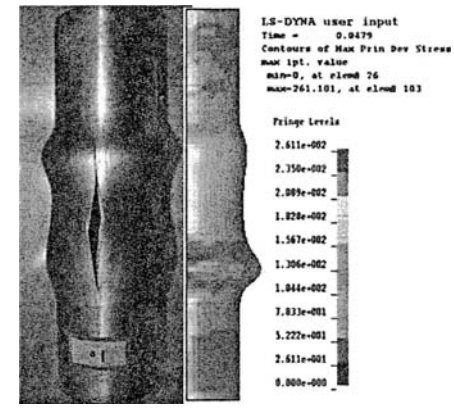

Fig. 12. Experimental and numerical predictions of bursting in a specimen with axial feeding + internal pressure.

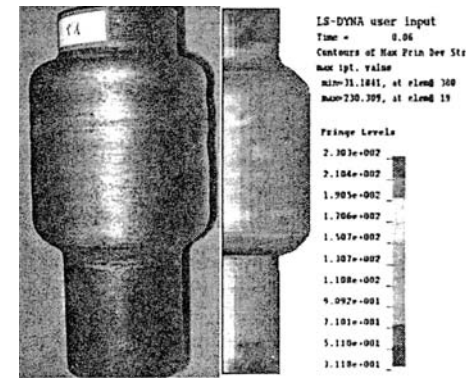

Fig. 13. Experimental and numerical predictions of a successful calibration with a cavity diameter of 60mm.

Table 1. The experimental and numerical data at the onset of failure for different loading paths.

Fig. no.	10(only feeding)	11(only pressure)	12(Feeding+ pressure)	13(feeding+ pressure)
Experiment	19 mm	35 MPa	30 MPa	65MPa, 30mm
Simulation	18.12 mm	34.15 MPa	27.5 MPa	60 MPa, 30mm

the internal pressure of the cases shown in Figs. 10 to 12 are given in Table 1. As can be seen in the Table, the experimental and the numerical results are very close, suggesting that the failure model adopted in this work is an appropriate one and that its constants have accurately been determined. The slight differences can be attributed to the errors in measuring devices and also to the failure model itself which is inherent with a constitutive relation based on experimental data.

5. Conclusions

From the experimental and numerical results, the following conclusions can be derived:

The numerical simulation can predict the failure as a consequence of buckling due to excessive axial feeding and bursting due to the excessive pressure or a combination of them.

Johnson-Cook material and failure models are appropriate if their constants are determined accurately.

Numerical simulations provide a cheap tool to examine the different parameters involved in THP which are usually very expensive and time consuming to be determined by experiment.

References

[1] Woo-Jin Song, Sang-Woo Kim, Jeong Kim, Beom-Soo Kang, Analytical and numerical analysis of bursting failure prediction in tube THP, *Journal of Materials Processing Technology.* 164-165 (2005) 1618-1623.

[2] Shijian Yuan, Wenjian Yuan and Xiaosong Wang, Effect of wrinkling behavior on formability and thick-ness distribution in tube THP, *Journal of Materials Processing Technology.* 177 (2006) 668-671.

[3] Shijian Yuan, Xiaosong Wang, gang Liu, Z.R. Wang, Control and use of wrinkles in tube THP, *Journal of Materials Processing Technology.* 182 (2007) 6-11.

[4] J.P. Abrantes, A. Szabo-Ponce, G.F. Batalha, Experimental and numerical simulation of tube THP (THF), *Journal of Materials Processing Technology.* 164-165 (2005) 1140-1147.

[5] H.Y. Li, X.S. Wang, S.J. Yuan, Q.B. Miao, Z.R. Wang, Typical stress state of tube THP and their distribution on the yield ellipse, *Journal of Materials Processing Technology.* 151 (2004) 345-349.

[6] Yang Lianfa and Gua Cheng, A simple experimental tooling with internal pressure source used for evaluation of material formability in tube THP, *Journal of Materials Processing Technology.* 180 (2006) 310-317.

[7] S. J. Yuan, G. Liu, X. R. Huang, X. S. Wang, W. C. Xie and Z. R. Wang, THP of typical hollow components, *Journal of Materials Processing Technology.* 151 (2004) 203-207.

[8] Lihui Lang, Shijian Yuan, Xiaosong Wang, Z. R. Wang, Zhuang Fu, J. Danckert and K. B. Nielsen, A study on numerical simulation of THP of aluminum alloy tube, *Journal of Materials Processings Technology.* 146 (2004) 377-388.